Supplementary Information

Superconducting Ce_2P_3 and CeP_2 with an interesting planar P layer

Xing Li[1], Aitor Bergara[2,3,4], Xiaohua Zhang[1], Fei Li[1], Yong Liu[1], and Guochun Yang[1*]

[1]State Key Laboratory of Metastable Materials Science & Technology and Key Laboratory for Microstructural Material Physics of Hebei Province, School of Science, Yanshan University, Qinhuangdao 066004, China

[2]Physics Department and EHU Quantum Center, Universidad del País Vasco-Euskal Herriko Unibertsitatea, UPV/EHU, 48080 Bilbao, Spain

[3]Donostia International Physics Center (DIPC), 20018 Donostia, Spain

[4]Centro de Física de Materiales CFM, Centro Mixto CSIC-UPV/EHU, 20018 Donostia, Spain

*Corresponding Authors E-mail: yanggc468@nenu.edu.cn; yanggc@ysu.edu.cn

Index **Page**

Computational Details

The structure prediction method was based on a global minimization of free energy surfaces combining ab initio total energy calculations, as implemented in the CALYPSO (Crystal Structure AnaLYsis by Particle Swarm Optimization) code.[1, 2] The structures of Ce_xP_y (x = 1, y = 0.5, 1, 1.5, 2-7; x = 3, y = 1-2) were searched with simulation cell sizes of 1-4 formula units (f.u.) at the selected pressures of 1 atm, and 25, 50, 100, 200, and 300 GPa. In the first step, random structures with certain symmetry were constructed, where atomic coordinates were generated by crystallographic symmetry operations. Local optimizations[3] using the VASP code were done with the conjugate gradients method and stopped when enthalpy changes became smaller than 1×10^{-5} eV per cell. After processing the first generation structures, 60% of them with lower enthalpies were selected to construct the next generation with PSO (Particle Swarm Optimization). 40% of the structures in the new generation were randomly generated. A structure fingerprinting technique of bond characterization matrix was applied to the generated structures, so that identical structures were strictly forbidden. These procedures significantly enhanced the diversity of the structures, which was crucial for structural global search efficiency. In most cases, structural searching simulations for each calculation were stopped after generating 1000 ~ 1200 structures (e.g., about 20 ~ 30 generations).

To further analyze the structures with higher accuracy, we selected a number of structures with lower enthalpies and perform a structural optimization using density functional theory within the generalized gradient approximation as implemented in the VASP code.[4] In all the calculations, the cutoff energy for the expansion of wavefunctions in plane waves was set to 600 eV, and the Monkhorst-Pack k-mesh with a grid spacing of $2\pi \times 0.03$ Å^{-1} was selected to meet the energy convergence within ~1 meV/atom. The electron-ion interaction was described by projector-augmented-wave potentials with $5s^2 5p^6 4f^1 5d^1 6s^2$ and $3s^2 3p^3$ configurations treated as valence electrons for Ce and P atoms, respectively.

Bonding was investigated by the crystal orbital Hamiltonian population (COHP) analysis using the LOBSTER code,[5] which provides an atom-specific measure of the bonding character of states in a given energy region, and the strength and origin of interatomic interactions can be obtained through the output file "COHPCAR.lobster. The Bader charge analysis[6] was used to determine charge transfer by analyzing the output file "ACF.dat". The electron localization function (ELF) was used to describe and visualize chemical bonds in stable compounds,[7] which is achieved by putting the output file "ELFCAR" into the VESTA software.[8] The phonon calculations were carried out by using supercell finite-displacement method as implemented in the PHONOPY code.[9] The electron-phonon coupling calculations were carried out with the density functional perturbation theory as executed in the QUANTUM ESPRESSO package.[10] We employed

the pseudopotentials with Ce.pbe-spdn-rrkjus_psl.1.0.0.UPF and P.pbe-n-rrkjus_psl.0.1.UPF for Ce and P atoms in *Pmma* Ce_2P_3, and Ce.pz-sp-hgh.UPF and P.pz-n-rrkjus_psl.0.1.UPF for Ce and P atoms in *P*6/*mmm* CeP_2, respectively. The considered kinetic energy cutoff and width were 70 Ry and 0.02 Ry, respectively. To reliably calculate the electron-phonon coupling in metallic systems we need to sample dense *k*-meshes for electronic Brillouin zone integration and enough *q*-meshes for evaluating average contributions from the phonon modes. Depending on the specific structures of the stable compounds, different *k*-meshes and *q*-meshes were used: 6 × 9 × 8 *k*-meshes and 2 × 3 × 4 *q*-meshes for Ce_2P_3 in the *Pmma* structure at 100, 75 and 50 GPa, 18 × 18 × 18 *k*-meshes and 6 × 6 × 6 *q*-meshes for CeP_2 in the *P*6/*mmm* structure at 16.5, 11, 5.5, and 0 GPa. We have calculated the superconducting T_c of Ce-P compounds as estimated from the McMillan-Allen-Dynes formula:[11]

$$T_c = \frac{\omega_{log}}{1.2} exp\left[-\frac{1.04(1 + \lambda)}{\lambda - \mu^*(1 + 0.62\lambda)} \right].$$

Here, μ^* is the Coulomb pseudopotential ($\mu^* = 0.1$). In addition, the EPC parameter, λ, and the logarithmic average phonon frequency, ω_{log} were calculated via the Eliashberg spectral function for the electron-phonon interaction:

$$\alpha^2F(\omega) = \frac{1}{N(E_F)} \sum_{kq,v} |g_{k,k+q,v}|^2 \delta(\varepsilon_k)\delta(\varepsilon_{k+q})\delta(\omega - \omega_{q,v}),$$

where $\lambda = 2\int d\omega \frac{\alpha^2F(\omega)}{\omega}$; $\omega_{log} = exp\left[\frac{2}{\lambda}\int \frac{d\omega}{\omega}\alpha^2F(\omega) ln(\omega)\right]$. Here, $N(E_F)$ is the electronic density of states at the Fermi level, $\omega_{q,v}$ is the phonon frequency of mode v and wave vector q, and $|g_{k,k+q,v}|$ is the electron-phonon matrix element between two electronic states with momenta k and $k + q$ at the Fermi level.[12, 13]

The temperature dependence of the superconducting gap (Δ) of CeP_2 at 0 GPa is explored. The electronic-phonon interpolation technique applied in the electron-phonon Wannier (EPW) code,[14] which is based on the maximum localized Wannier function, is an efficient and accurate method to calculate the superconducting gaps and T_c. The width of the Fermi surface window is set 0.15 eV and the Dirac δ functions are replaced by Lorentzians of widths (σ) 0.025 eV and 0.1 meV for electrons and phonons, respectively. The precedent computations of the electronic wave functions required for the Wannier interpolations are carried out within a uniform unshifted BZ k-mesh of 6 × 6 × 6. An interpolated k-point grid of 72 × 72 × 72 and q-point grid of 24 × 24 × 24 are set to solve the anisotropic Migdal-Eliashberg equations. The fermion Matsubara

frequencies cutoff is set to be 1 eV, a reasonable setting is 4 times higher than the largest phonon frequency, our setting is 10 times higher. The Morel-Anderson pseudopotential μ_c^* is set 0.13.

Supplementary Figures

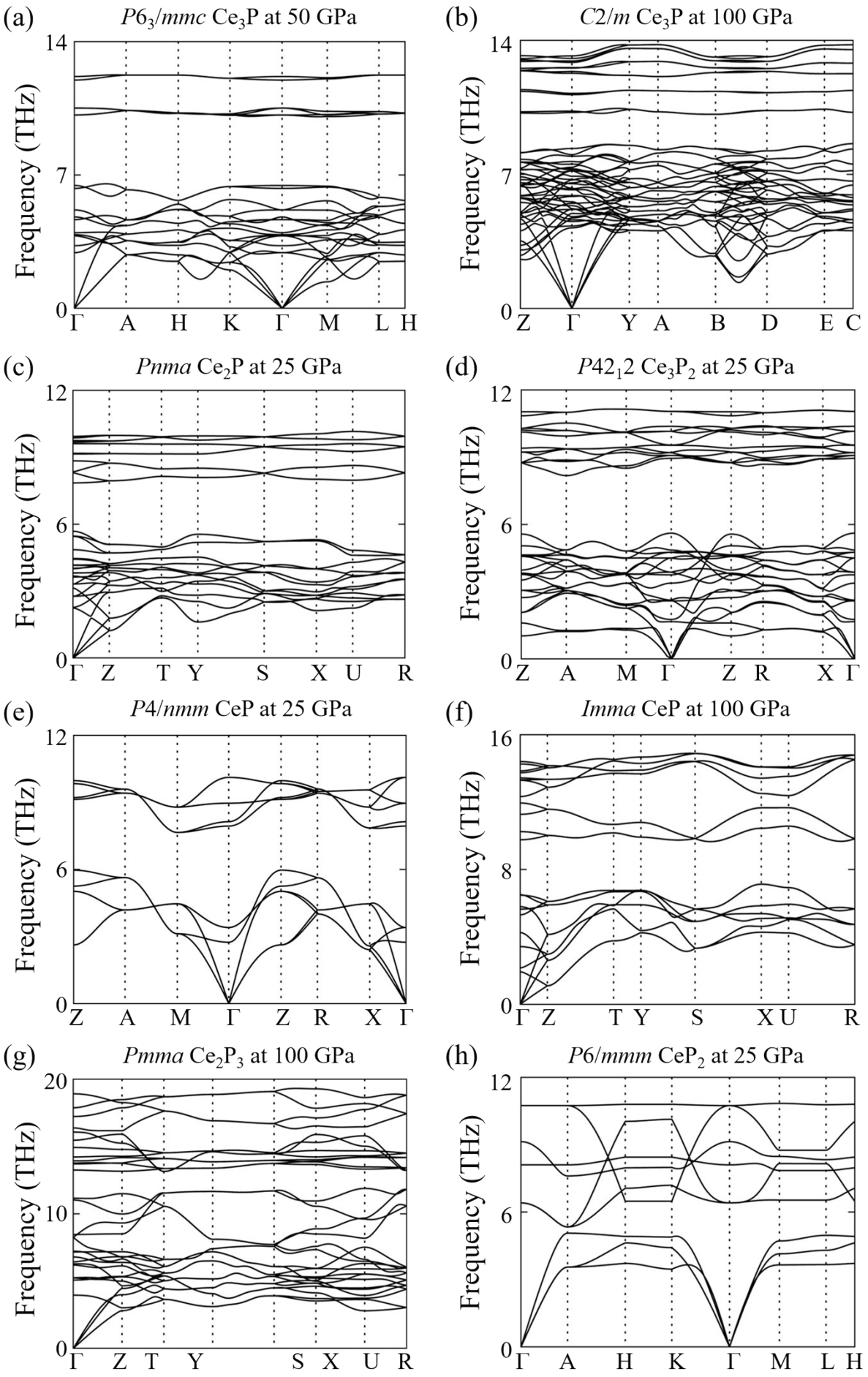
(a)
$P6_3/mmc$ Ce_3P at 50 GPa
Frequency (THz)
14
7
0
Γ A H K Γ M L H
(b)
$C2/m$ Ce_3P at 100 GPa
Frequency (THz)
14
7
0
Z Γ Y A B D E C
(c)
$Pnma$ Ce_2P at 25 GPa
Frequency (THz)
12
6
0
Γ Z T Y S X U R
(d)
$P42_12$ Ce_3P_2 at 25 GPa
Frequency (THz)
12
6
0
Z A M Γ Z R X Γ
(e)
$P4/nmm$ CeP at 25 GPa
Frequency (THz)
12
6
0
Z A M Γ Z R X Γ
(f)
$Imma$ CeP at 100 GPa
Frequency (THz)
16
8
0
Γ Z T Y S X U R
(g)
$Pmma$ Ce_2P_3 at 100 GPa
Frequency (THz)
20
10
0
Γ Z T Y S X U R
(h)
$P6/mmm$ CeP_2 at 25 GPa
Frequency (THz)
12
6
0
Γ A H K Γ M L H

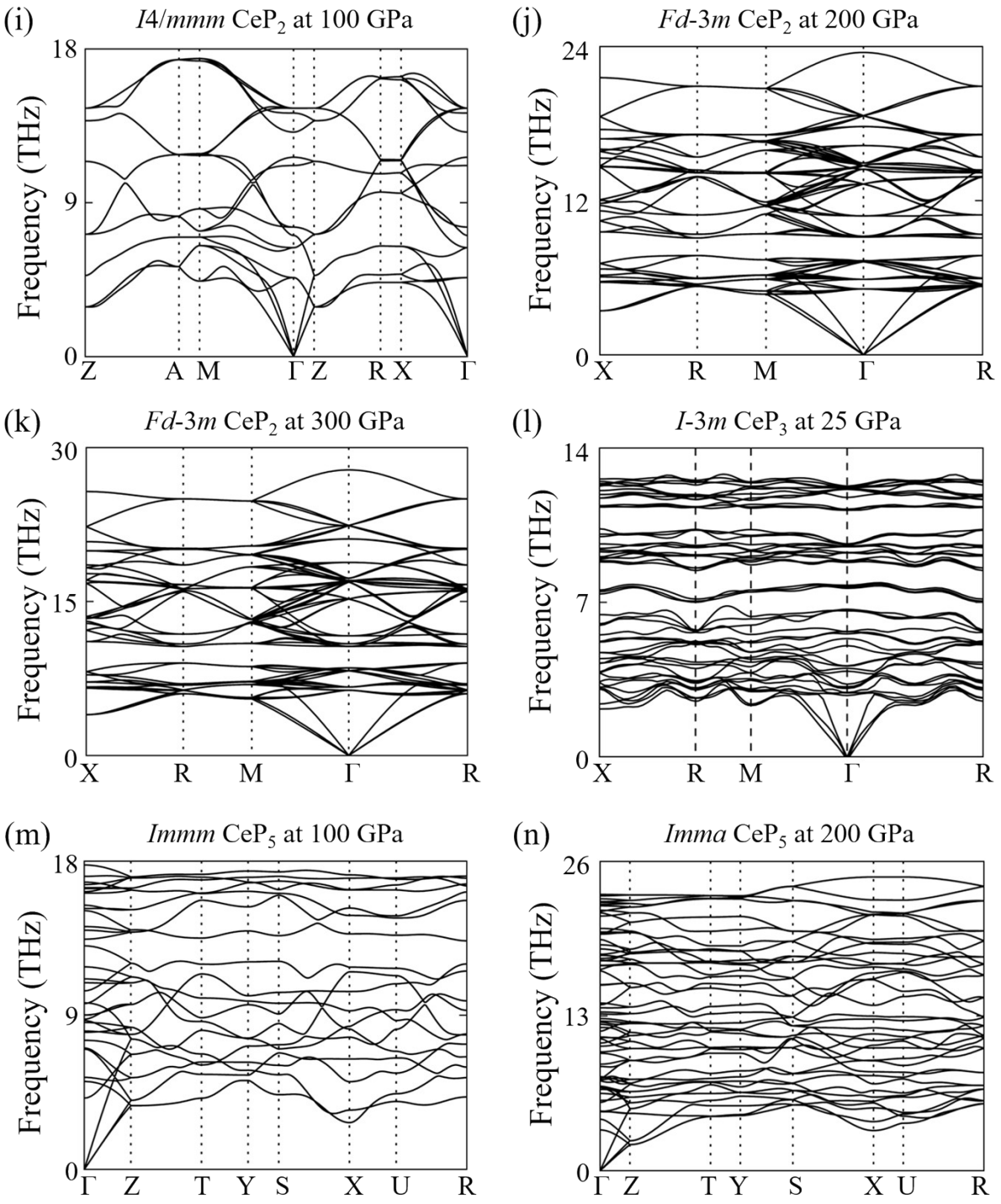

Fig. S1. Phonon dispersion curves of the stable Ce-P compounds.

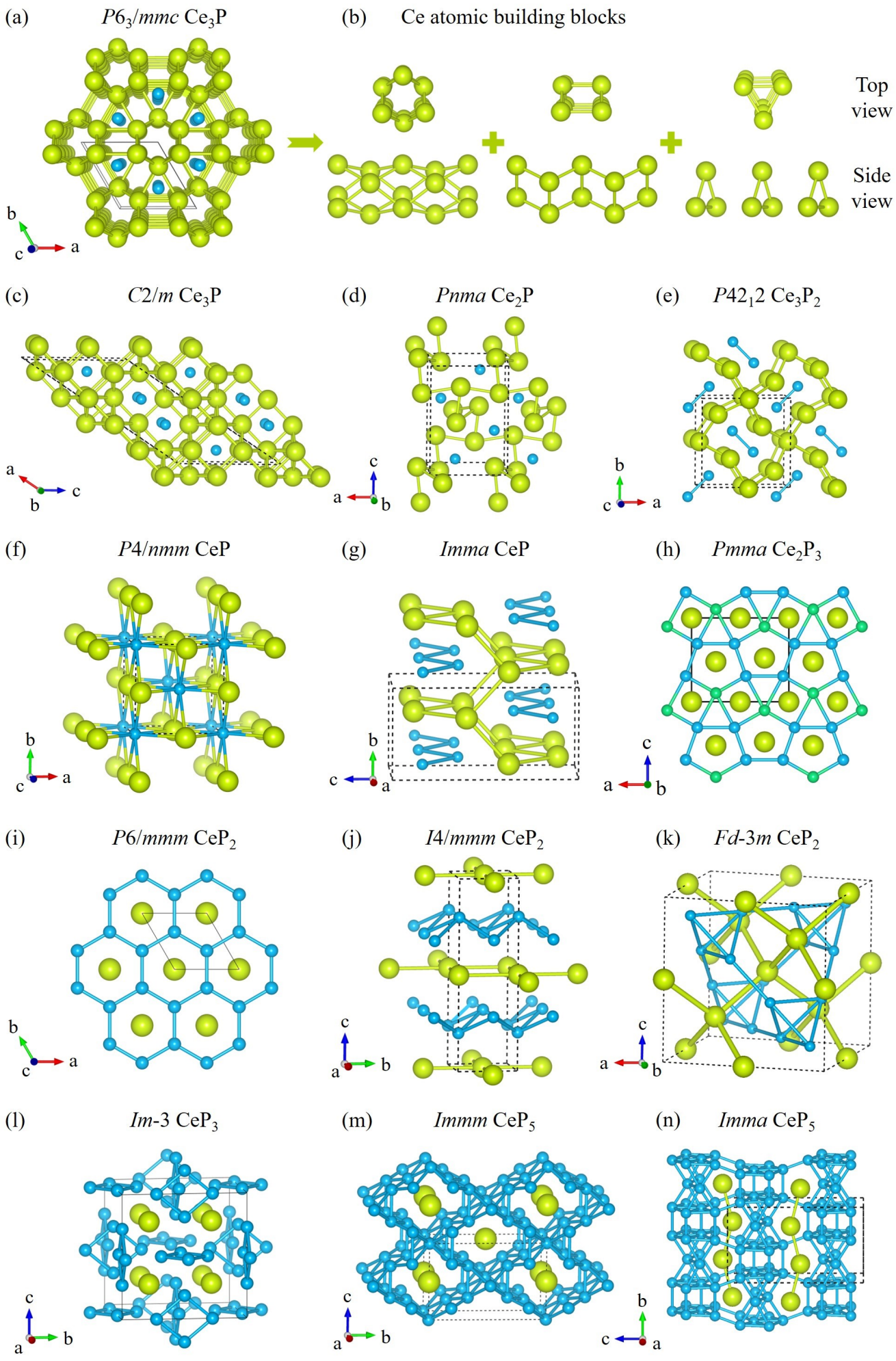
(a) $P6_3/mmc$ Ce_3P
(b) Ce atomic building blocks
Top view
Side view
(c) $C2/m$ Ce_3P
(d) $Pnma$ Ce_2P
(e) $P42_12$ Ce_3P_2
(f) $P4/nmm$ CeP
(g) $Imma$ CeP
(h) $Pmma$ Ce_2P_3
(i) $P6/mmm$ CeP_2
(j) $I4/mmm$ CeP_2
(k) Fd-3m CeP_2
(l) Im-3 CeP_3
(m) $Immm$ CeP_5
(n) $Imma$ CeP_5

Fig. S2. The crystal structures of the stable Ce-P compounds.

For these Ce-P compounds, the degree of aggregation of the P atomic structural units increases with P content, which changes from a single atom in *C*2/*m* Ce_3P, *P*6$_3$/*mmc* Ce_3P, and *Pnma* Ce_2P, to a dimer in *P*42$_1$2 Ce_3P_2, to a zigzag chain in *Imma* CeP, to a wrinkled layer in *I*4/*mmm* CeP_2 or planar layer in *Pmma* Ce_2P_3 and *P*6/*mmm* CeP_2, and, eventually, to a three-dimensional framework in *Fd*-3*m* CeP_2 and *Immm*/*Imma* CeP_5. The same variation trend can be found with increasing the Ce content. The crystal structure of *Im*-3 CeP_3 can be considered a new skutterudite-like compound. More interestingly, it shows dynamical stability and superconductivity at ambient pressure, which will be discussed in detail elsewhere.

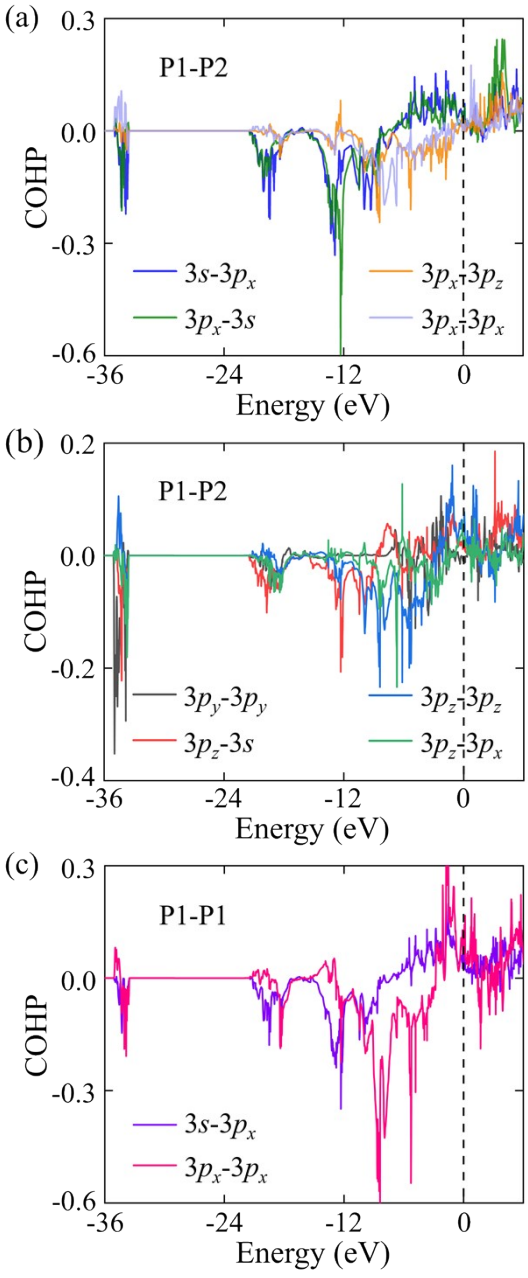

Fig. S3. The COHP of (a) the shortest P1-P2 pair and (b-c) the longest P1-P1/P2 pair in *Pmma* Ce_2P_3 at 100 GPa.

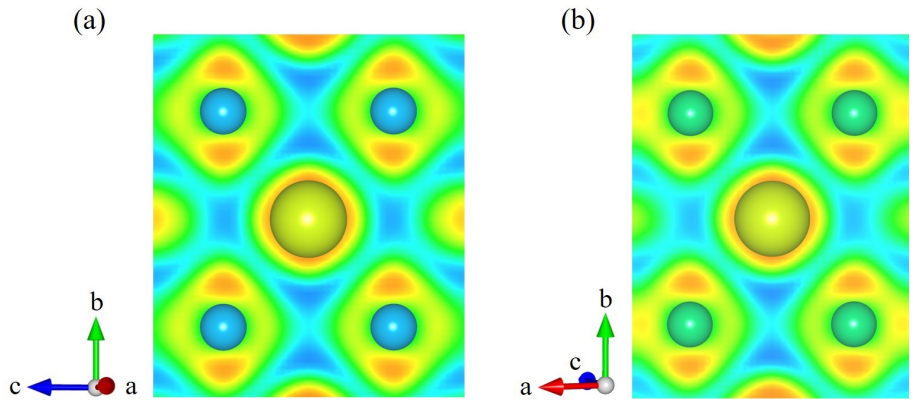

Fig. S4. The ELF maps of *Pmma* Ce_2P_3 at 100 GPa.

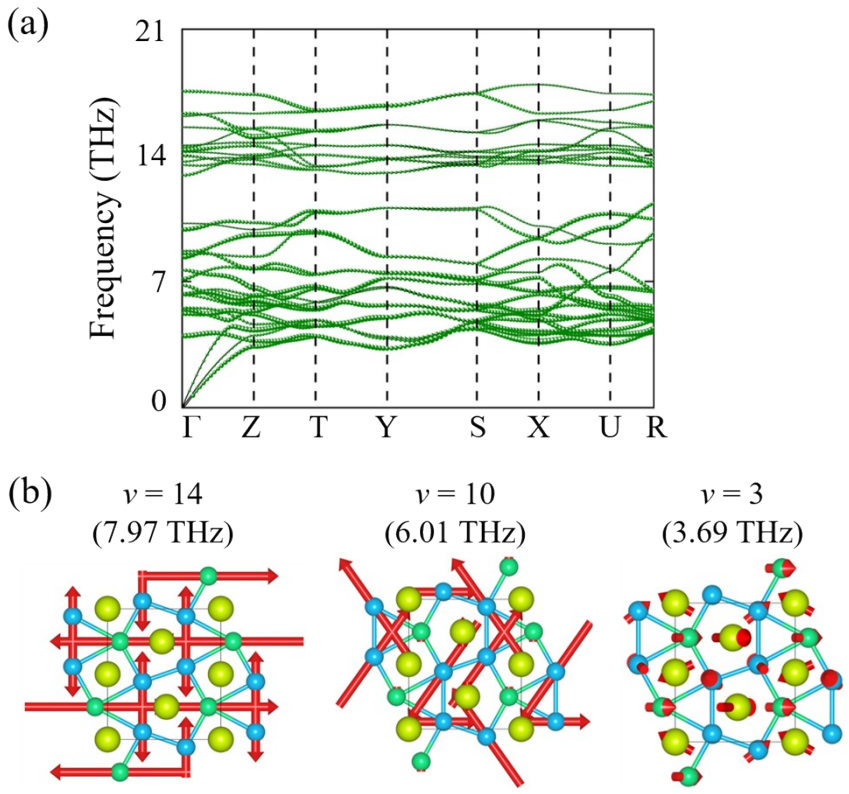

Fig. S5. (a) The phonon dispersion curves (the magnitude of λ is indicated by the thickness of the green curves), and (b) main vibrational modes contributing to the superconductivity of *Pmma* Ce_2P_3 at 100 GPa, where *v* represents the sequence number of the phonon curve from bottom to top.

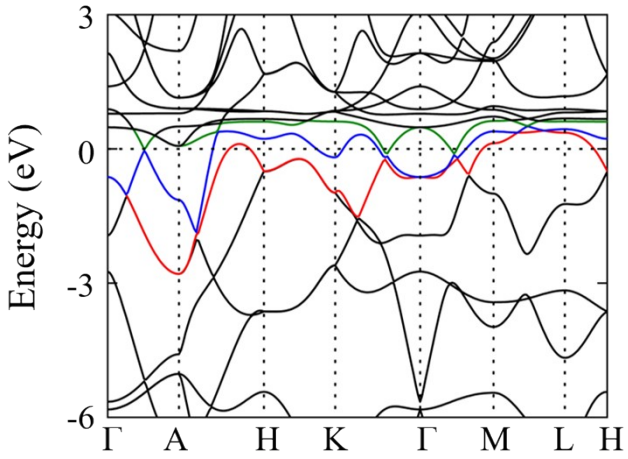

Fig. S6. The electronic band structure of *P*6/*mmm* CeP_2 at 0 GPa.

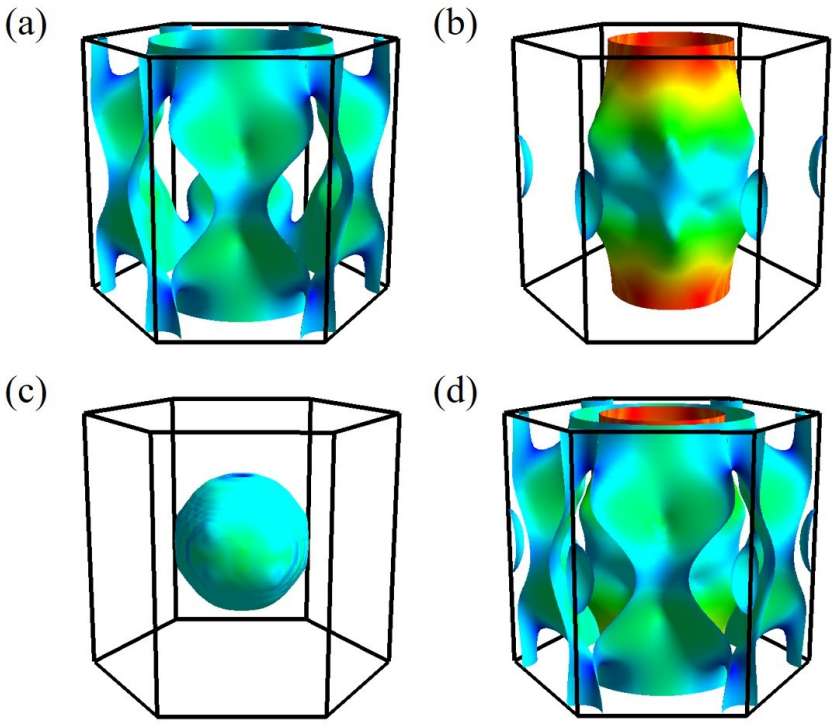

Fig. S7. (a-c) The Fermi surfaces associated to bands crossing the Fermi level of *P*6/*mmm* CeP_2 at 0 GPa, and (d) the side view of merged Fermi surfaces.

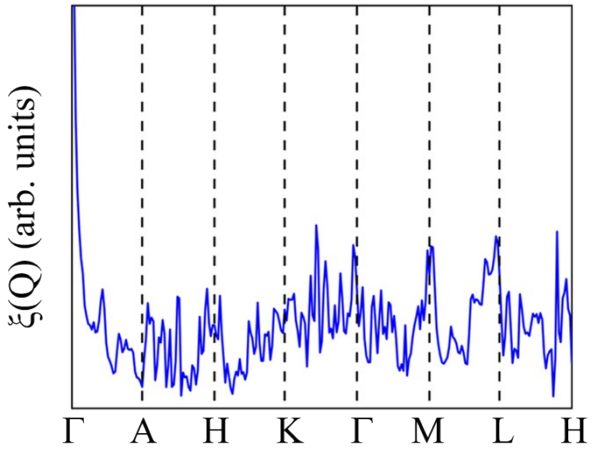

Fig. S8. The Fermi surface nesting function ξ (Q) of *P*6/*mmm* CeP_2 at 0 GPa.

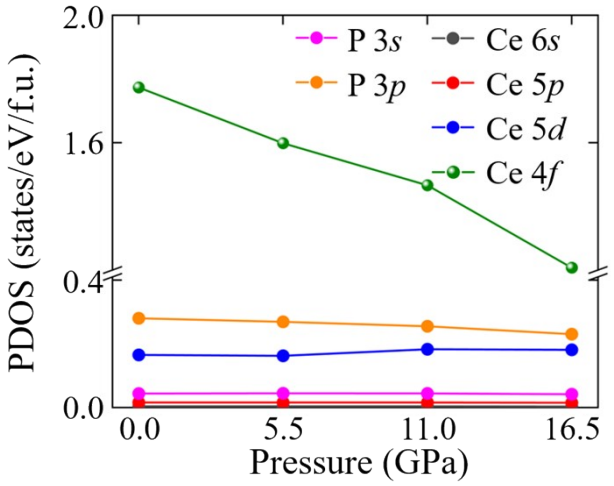

Fig. S9. Pressure-dependent projected density of states (PDOS) of *P*6/*mmm* CeP_2.

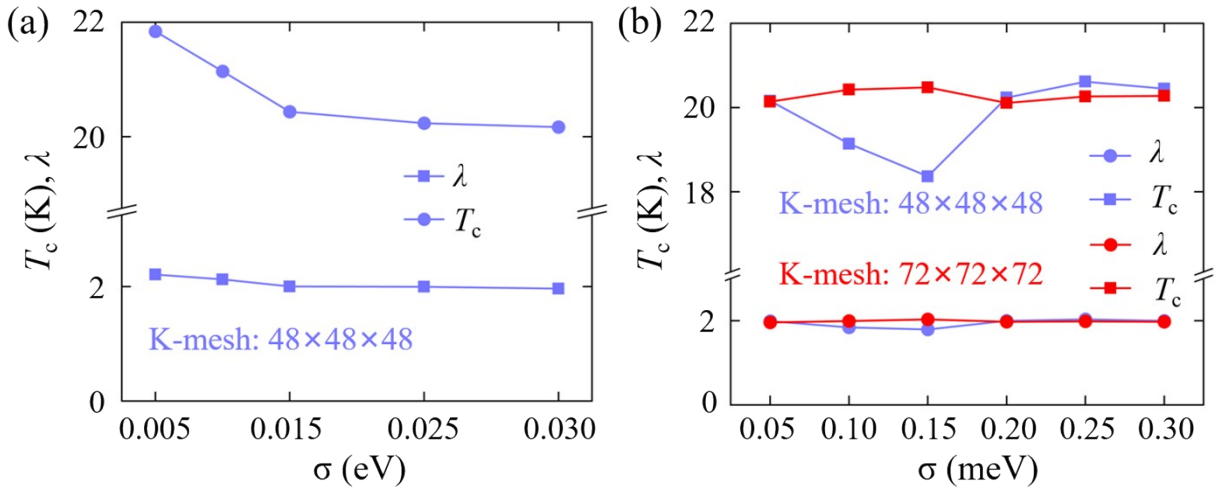

Fig. S10. Convergence tests of the λ and T_c versus different smearing parameters σ for (a) electrons and (b) phonons in *P*6/*mmm* CeP_2. Here, we choose 0.025 eV and 0.1 meV for electrons and phonons due to their good convergence.

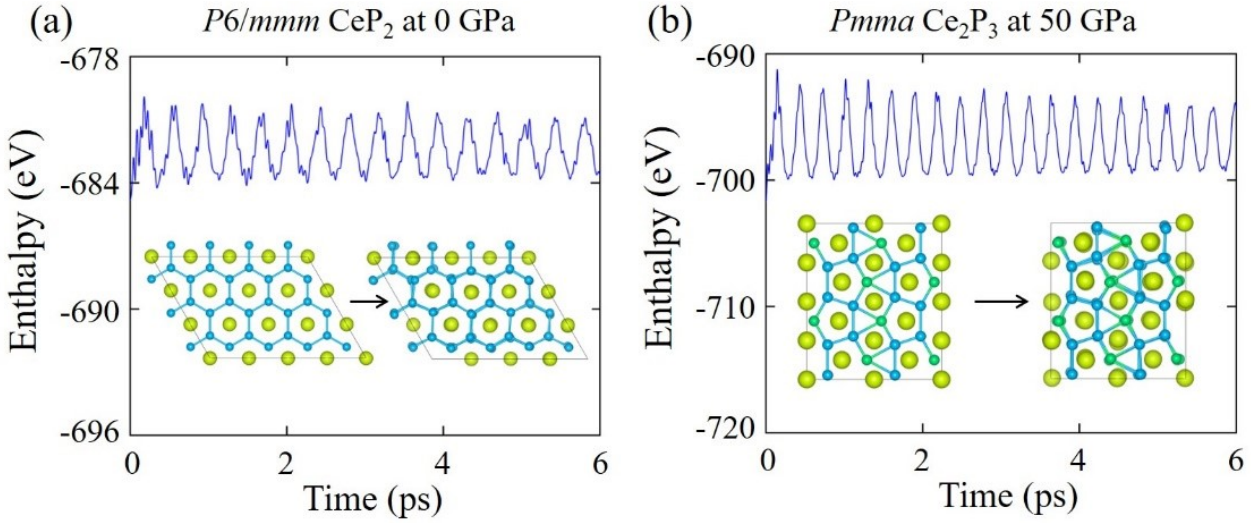

Fig. S11. Evolution of total enthalpy and snapshots of the (a) *P6/mmm* CeP_2 and (b) *Pmma* Ce_2P_3 at 300 K from AIMD simulations.

Supplementary Tables

Table S1. Length and ICOHP of the Ce/La-P pair and volumes of *P6/mmm* CeP_2 and LaP_2 at 0 GPa.

Phase	Pressure (GPa)	Volume ($Å^3$)	Length of Ce-P pair (Å)	ICOHP of Ce-P pair (eV/Pair)	Length of La-P pair (Å)	ICOHP of La-P pair (eV/Pair)
P6/mmm CeP_2	0	49.946	2.928	-1.152	-	-
P6/mmm LaP_2	0	62.679	-	-	3.170	-0.615

Table S2. Structural information of the predicted stable Ce-P phases.

Phases	Pressure (GPa)	Lattice Parameters (Å,°)	Wyckoff Positions (fractional)			
			atoms	x	y	z
Pnma Ce_2P	25	a = 5.7653	Ce(4c)	-0.8443	0.7500	0.0463
		b = 4.5319	P(4c)	-0.3959	0.7500	0.7789
		c = 8.2786	P(4c)	-0.6645	0.2500	0.8811
		α = 90.0000				
		β = 90.0000				
		γ = 90.0000				

$P42_12$ Ce_3P_2	25	a = 6.9857	Ce(4e)	0.1800	0.8200	0.0000
		b = 6.9857	Ce(2c)	0.5000	0.0000	0.4050
		c = 3.7241	P(4f)	0.3831	0.6169	0.5000
		α = 90.0000				
		β = 90.0000				
		γ = 90.0000				
*P*4/*nmm* CeP	25	a = 4.6468	Ce(2c)	0.5000	0.0000	0.5537
		b = 4.6468	P(2a)	0.0000	0.0000	0.0000
		c = 3.2310				
		α = 90.0000				
		β = 90.0000				
		γ = 90.0000				
*P*6/*mmm* CeP_2	25	a = 3.8905	Ce(1a)	0.0000	0.0000	0.0000
		b = 3.8905	P(2d)	0.3333	0.6667	0.5000
		c = 3.6106				
		α = 90.0000				
		β = 90.0000				
		γ = 120.0000				
$P6_3/mmc$ Ce_3P	50	a = 5.8199	Ce(6h)	0.1724	-1.6552	1.2500
		b = 5.8199	P(2d)	0.6667	-0.6667	1.2500
		c = 4.3824				
		α = 90.0000				
		β = 90.0000				
		γ = 120.0000				
Pmma Ce_2P_3	50	a = 6.3402	Ce(2a)	1.0000	0.0000	0.0000
		b = 4.1236	Ce(2e)	0.7500	0.0000	0.5215
		c = 5.4803	P(2f)	1.2500	0.5000	0.1089
		α = 90.0000	P(4j)	1.0544	0.5000	0.6903
		β = 90.0000				
		γ = 90.0000				
*C*2/*m* Ce_3P	100	a = 13.7598	Ce(4i)	0.8786	0.0000	0.1950
		b = 3.7713	Ce(4i)	0.1279	0.0000	0.3242
		c = 7.6586	Ce(4i)	0.8724	0.5000	0.9358
		α = 90.0000	P(4i)	0.1228	0.5000	0.5651
		β = 146.5235				
		γ = 90.0000				
Imma CeP	100	a = 3.2448	Ce(4e)	0.5000	0.7500	0.6133
		b = 3.9626	P(4e)	0.0000	0.2500	0.6500
		c = 7.8986				
		α = 90.0000				
		β = 90.0000				
		γ = 90.0000				

*I*4/*mmm* CeP_2	100	a = 2.7904	Ce(2b)	0.5000	0.5000	0.0000
		b = 2.7904	P(4e)	0.0000	0.0000	0.8002
		c = 8.9938				
		α = 90.0000				
		β = 90.0000				
		γ = 90.0000				
Immm CeP_5	100	a = 3.3249	Ce(2c)	0.0000	0.0000	0.5000
		b = 7.6728	P(8l)	0.0000	0.3307	0.7082
		c = 5.0409	P(2a)	0.0000	0.0000	0.0000
		α = 90.0000				
		β = 90.0000				
		γ = 90.0000				
Fd-3*m* CeP_2	200	a = 6.1258	Ce(8b)	0.0000	0.0000	0.5000
		b = 6.1258	P(16c)	0.1250	0.1250	0.1250
		c = 6.1258				
		α = 90.0000				
		β = 90.0000				
		γ = 90.0000				
Imma CeP_5	200	a = 3.7001	Ce(4e)	0.5000	1.2500	0.0358
		b = 5.6806	P(4e)	0.0000	0.7500	0.7954
		c = 10.0278	P(8h)	0.0000	0.5614	0.0927
		α = 90.0000	P(8h)	0.0000	1.0763	0.6941
		β = 90.0000				
		γ = 90.0000				

Table S3. Elastic constants of *P*6/*mmm* CeP_2 at 0 GPa and *Pmma* Ce_2P_3 at 50 GPa.

*P*6/*mmm* CeP_2		*Pmma* Ce_2P_3	
C11 (N/m)	215.548	C11 (N/m)	334.810
C12 (N/m)	121.984	C12 (N/m)	146.028
C13 (N/m)	87.355	C13 (N/m)	33.135
C33 (N/m)	276.864	C22 (N/m)	410.442
C44 (N/m)	83.353	C23 (N/m)	167.417
C66 (N/m)	46.782	C33 (N/m)	314.640
		C44 (N/m)	227.514
		C55 (N/m)	137.698
		C66 (N/m)	209.870

References

1 Y. Wang, J. Lv, L. Zhu and Y. Ma, *Phys. Rev. B*, 2010, **82**, 094116.

2 Y. Wang, J. Lv, L. Zhu and Y. Ma, *Comput. Phys. Commun.*, 2012, **183**, 2063-2070.

3 G. Kresse and J. Furthmüller, *Phys. Rev. B*, 1996, **54**, 11169.

4 J. Hafner, *J. Comput. Chem.*, 2008, **29**, 2044-2078.
5 R. Nelson, C. Ertural, J. George, V. L. Deringer, G. Hautier and R. Dronskowski, *J. Comput. Chem.*, 2020, **41**, 1931-1940.
6 W. Tang, E. Sanville and G. Henkelman, *J. Phys.: Condens. Matter*, 2009, **21**, 084204.
7 A. D. Becke and K. E. Edgecombe, *J. Chem. Phys.*, 1990, **92**, 5397-5403.
8 K. Momma and F. Izumi, *J. Appl. Cryst.*, 2011, **44**, 1272-1276.
9 S. Baroni, S. de Gironcoli, A. Dal Corso and P. Giannozzi, *Rev. Mod. Phys.*, 2001, **73**, 515-562.
10 P. Giannozzi, S. Baroni, N. Bonini, M. Calandra, R. Car, C. Cavazzoni, D. Ceresoli, G. L. Chiarotti, M. Cococcioni and I. Dabo, *J. Phys: Condens. Matter*, 2009, **21**, 395502.
11 P. B. Allen and R. C. Dynes, *Phys. Rev. B*, 1975, **12**, 905.
12 J. P. Carbotte, *Rev. Mod. Phys.*, 1990, **62**, 1027.
13 P. B. Allen and B. Mitrović, *Solid State Phys.*, 1983, **37**, 1-92.
14 S. Poncé, E. R. Margine, C. Verdi and F. Giustino, *Comput. Phys. Commun.*, 2016, **209**, 116-133.